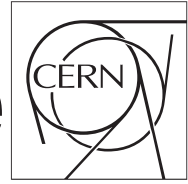


The Compact Muon Solenoid Experiment

CMS Draft Note

Mailing address: CMS CERN, CH-1211 GENEVA 23, Switzerland



2013/08/07

Head Id: 167902

Archive Id: 201321

Archive Date: 2013/01/28

Archive Tag: trunk

Performance Study of L1 Calorimeter Trigger for Heavy Ion Collisions with High Luminosity

The CMS Collaboration

Abstract

This box is only visible in draft mode. Please make sure the values below make sense.

PDFAuthor: Alex Barbieri, Yen-Jie Lee, Wei Li, Matthew Nguyen, Christof Roland
PDFTitle: Performance Study of L1 Calorimeter Trigger for Heavy Ion Collisions with High Luminosity
PDFSubject: CMS
PDFKeywords: CMS, physics, software, computing

Please also verify that the abstract does not use any user defined symbols

High-energy collisions of heavy ions allow studies of the quark-gluon plasma (QGP) which consists of an extended volume of deconfined and chirally-symmetric quarks and gluons. The focus of the CMS heavy ion program is on the measurements of high p_T probes such as jets, photons, muons and electrons produced with the QGP which exploits the excellent capability of the CMS detector. The high statistics PbPb run at nominal center-of-mass energy of 5.5 TeV in 2015 will allow detailed studies on b-jet quenching, multi-jet events and azimuthal anisotropy of high p_T jets and tracks which provide important constraints of parton energy loss mechanism in QGP.

To optimize the high p_T physics reach, the level-1 trigger system was adapted to select collisions with potential high p_T physics signatures while applying prescales to minimum bias events already at the level-1 to conserve readout bandwidth. Due to the large underlying event fluctuation, the current level-1 trigger system of CMS provides only limited selectivity to jets in the high density heavy-ion background, a factor of 2 rejection factor over min bias collisions was achieved. Combined with a maximum readout rate of 3 kHz this allowed the CMS trigger and readout system to fully exploit high p_T physics up to an interaction rate of 6 kHz.

PbPb data taking at collisions rate above the 4.5 kHz maximal rate achieved in 2011 requires an upgrade of the present detector capabilities. During the PbPb run in 2015, at least a factor of 2-4 increase in the instantaneous luminosity is expected. Furthermore, the rate of high p_T probes will increase by roughly a factor of 5, due to the expected increase of the collisions energy by about a factor of 2. The future CMS heavy-ion physics program will continue to rely on highly selective online triggers, such as the single track, photon, jet and muon triggers deployed in the first two heavy-ion runs. Currently, the overall selectivity of the trigger system at the highest luminosities is limited by the hardware-based level-1 system which does not allow an event-by-event subtraction of the underlying event for jet triggers (at the HLT, a jet algorithm with full background selection and energy correction is employed). This limits the rate with which jet production can be sample dead-time free to about twice the readout bandwidth limit of 2-3 kHz. A factor of 5-10 reduction on the level-1 trigger rate will be needed for all foreseeable increases in heavy-ion luminosities within the next decade. Therefore, a level 1 trigger system which allows event-by-event background subtraction for jet and single track triggers is required. This new system will need to be commissioned in 2015 to ensure successful PbPb data taking.

The studies in this technical note indicate that the required rejection factors for level-1 jet triggers could be achieved using an improved communication scheme in the level-1 decision logic, allowing the determination of an average background in rings of azimuth. The first step for such an upgrade could already be implemented in the 2013 shutdown.

1 Physics Motivation

Studies of jet production in the 2010 and 2011 PbPb data sets have helped to elucidate the nature of parton energy loss in hot nuclear matter [1, 2]. With the larger data samples expected in 2015 and beyond, we expect to be able to measure the as yet unobserved flavor dependence jet quenching, given jet triggers which are sufficiently selective. In this section we give rate estimates for two key measurements which are sensitive to flavor dependence: b-dijet asymmetry and 3-jet production.

A proof of principle measurement of b-jet production in PbPb collisions has been performed with the 2011 data. This measurement of the b-jet to inclusive jet ratio, however, suffers from large statistical and systematic uncertainties. The golden measurement in the b-jet channel

would be a measurement of the dijet asymmetry for doubly-tagged b-jets, where we expect systematic uncertainties to be small and mostly common with the corresponding light jet measurement. The rate of doubly-tagged b-jets has been estimated based on the number inclusive dijets in the 2011 sample. The b-jet to inclusive jet ratio was measured to be roughly 0.03 in pp collisions at 7 TeV, as well as in 2.76 TeV PbPb collisions, with significantly larger uncertainties in the latter case. Of these b-jets only about 20%, will be produced back-to-back with another b-jet, in the so-called flavor creation mode. Using a simple secondary vertex tagger, one can achieve about 50% tagging efficiency in PbPb. For doubly-tagged jets, then, one only obtains a tagging efficiency of 25%, but the purity will be close to unity. Assuming x_T scaling with an exponent of $n = 4.5$, the yield of jets at fixed p_T increases by a factor of 5. Figure 1 shows the A_J distribution from Pythia, where A_J is the difference in the leading and sub-leading jet transverse momenta divided by their sum, assuming an integrated luminosity of a factor 10 more than the 2011. The kinematic cuts on the leading and sub-leading jets are $p_T > 100$ GeV/c and $p_T > 30$ GeV/c, respectively, for jets in $|\eta| < 2$.

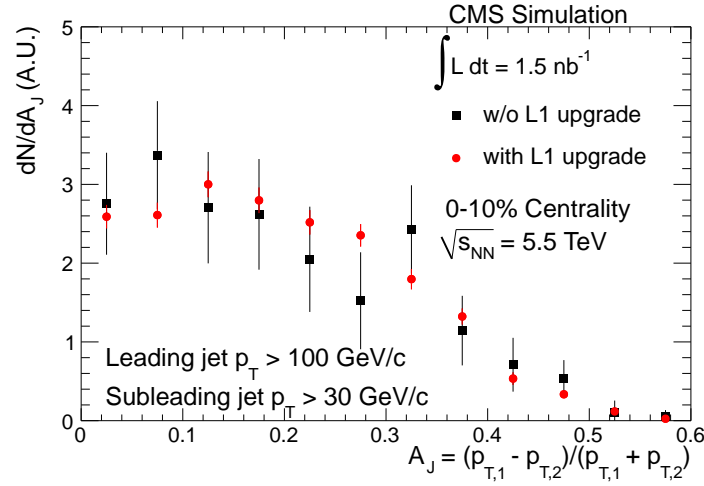


Figure 1: A_J distribution for doubly-tagged b-jets of $p_{T,1} > 100$ GeV/c, $p_{T,2} > 30$ GeV/c and $|\eta| < 2$ in the ten percent most central collisions expected in the 2015 PbPb Run.

The ratio of 3-jet to 2-jet events (R_{32}), is predicted based on the observed statistics in the 2011 data sample, in which we recorded about 106 3-jet events and 8225 dijet events with all jets having $p_T > 100$ GeV/c. The ratio from Pythia with the expected 2015 statistics is shown in Fig. 2.

2 Upgrade schemes

2.1 Current System

The current set of jet triggers, based on information from the L1 calorimeter trigger, is capable of reducing the trigger rate by a factor of 2 at the 2011 luminosity level without adverse physics effects. Because the level-1 jet triggers have a lot of overlap they do not respond well to increased thresholds or prescales. With the planned increase in luminosity after LS1, the jet trigger must have a reliable rejection factor of 95% on minimum bias data in order to stay within the I/O limits of the L1/HLT connection.

The current L1 trigger jet finder operates at the region level with no background subtraction. Each jet consists of 3x3 regions (each region is 4x4 towers), with the requirement that the middle

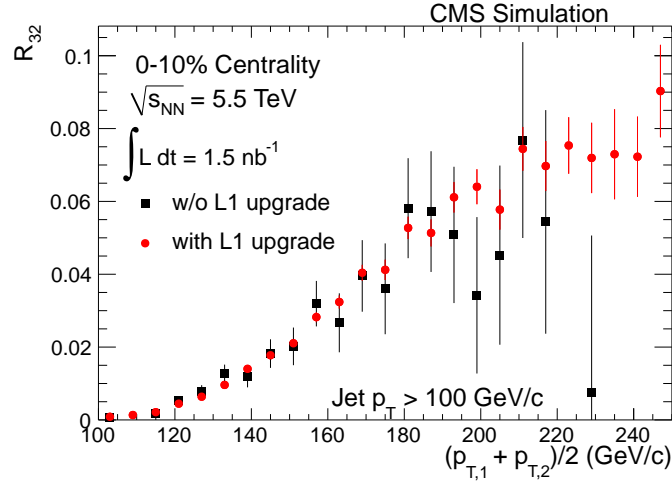


Figure 2: The ratio of 3-jet to 2-jet events as a function of the average p_T of the two leading jets for $p_T > 100$ GeV/c in the ten percent most central collisions expected in the 2015 PbPb Run.

region be a local maximum. Each leaf card (2x11 regions) sends its 6 largest jets to the wheel cards (half of the detector, $\pm\eta$) which orders the jets by E_T . The trigger threshold is applied to the largest jet of the event.

2.2 Alternative Algorithms using the Current System

Alternative algorithms using the existing system hardware were investigated. The investigated algorithms can be split into two categories: final jet list algorithms which use the information in the Global Calorimeter Trigger (GCT), and algorithms which use information available in the Regional Calorimeter Trigger (RCT).

Using the list of L1 jets available at the Global Calorimeter Trigger, subtracting the median or different quartiles of the list from the most energetic jet can be used as a background subtraction method before applying the threshold.

The RCT has available to it 2x11 regions covering $\Delta\phi = \pi/9$ and half the detector in η . Subtracting the minimum or mean region value in the RCT from each region can be used as a background subtraction method before applying the threshold.

2.3 2015 System (Wisconsin)

The proposed “2015” system replaces the current Global Calorimeter Trigger logic with a system that has access to the full $\eta - \phi$ map. With the full detector map a subtraction scheme which finds the average energy at each rapidity and subtracts this background is possible.

In this upgrade scheme the trigger logic still operates at the region level, in contrast to the SLHC system. This means that the leaf cards of the Calorimeter trigger do not need to be replaced.

2.4 SLHC System

The SLHC system operates at the tower level and allows background subtraction. Before jet-finding is run, the average E_T for a fixed eta is computed and subtracted from each tower with a 0 floor. The level-1 definition of a jet is flexible in the SLHC system, and for this study a jet consists of ‘circular’ groups of towers with a diameter of 7 towers for L1 Primitives data.

99 This shape was chosen to perform slightly better than the 2015 system in order to show the
 100 flexibility of the SLHC system.

101 3 Jet Trigger Performance

102 3.1 Alternative Algorithms

103 3.1.1 Jet List subtraction

104 An E_T -sorted list of L1 jets is available to the GCT; subtracting the first quartile of the jet list
 105 (more effective than the median or third quartile) from the largest jet could be used as a back-
 106 ground subtraction method. The results of using this method on the L1 accept rate are shown
 107 in Figs. 3, 4, 5. The increased luminosity after LS1 requires that the minimum bias rate must fall
 108 to 5% at the lowest unprescaled jet p_T , and the Figures show that even with jet list subtraction
 109 the required threshold is unreasonably high.

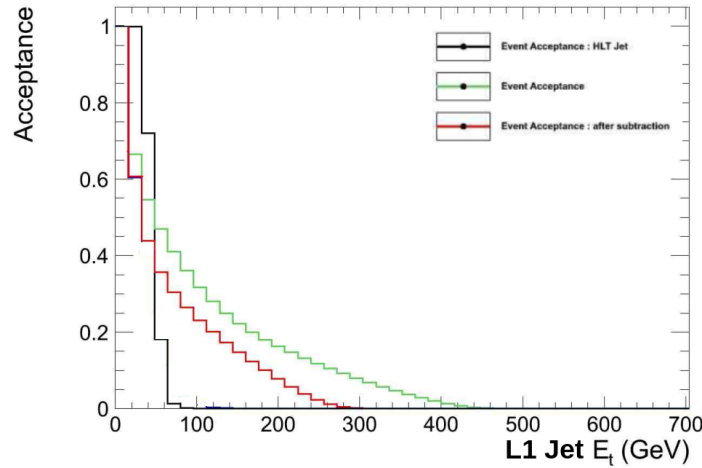


Figure 3: Comparison of accept rates before and after subtraction of the 1st quartile from the highest L1 jet. HLT jet shown as a reference. Minimum bias sample.

110 3.1.2 RCT level subtraction

111 Using only the information available in the leaf RCT cards, a section of the detector 2 regions
 112 wide in ϕ and 11 wide in η , the minimum or mean E_T of the regions can be subtracted. Unfor-
 113 tunately, in central events these methods perform poorly for reasons shown in Fig. 6, due to
 114 non-uniform response of the detector as a function of η and centrality.

115 Because of the high energy deposition at fixed values of eta in central collisions, effective back-
 116 ground subtraction methods must have access to the complete $\eta - \phi$ map of the detector.

117 3.2 Accept Rate

118 One measure of the performance of a trigger is the rejection rate and the response of the re-
 119 jection rate to increased threshold of the trigger. Figure 9 shows a comparison of the trigger
 120 systems' rejection rate as a function of the threshold set at level-1. With the luminosity increase
 121 after long shutdown 1, an accept rate of 5% is required in order to remain sample dead-time
 122 free.

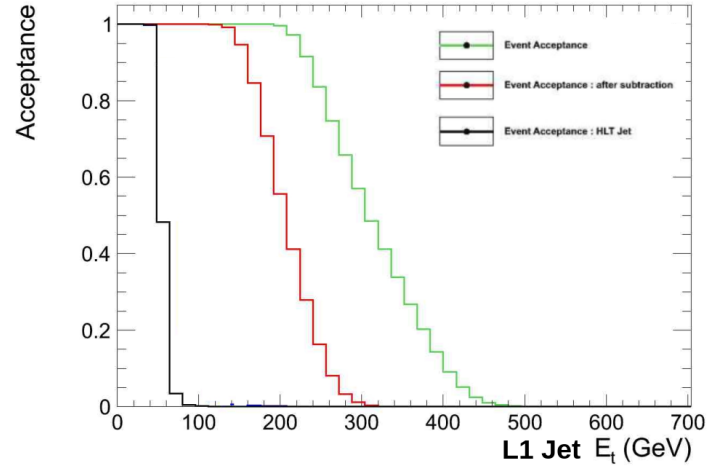


Figure 4: Comparison of accept rates before and after subtraction of the 1st quartile from the highest L1 jet. HLT jet shown as a reference. Central sample.

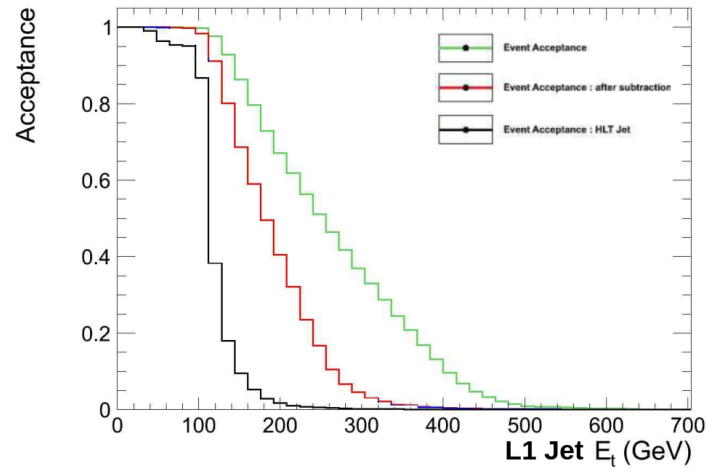


Figure 5: Comparison of accept rates before and after subtraction of the 1st quartile from the highest L1 jet. HLT jet shown as a reference. Jet 95 sample.

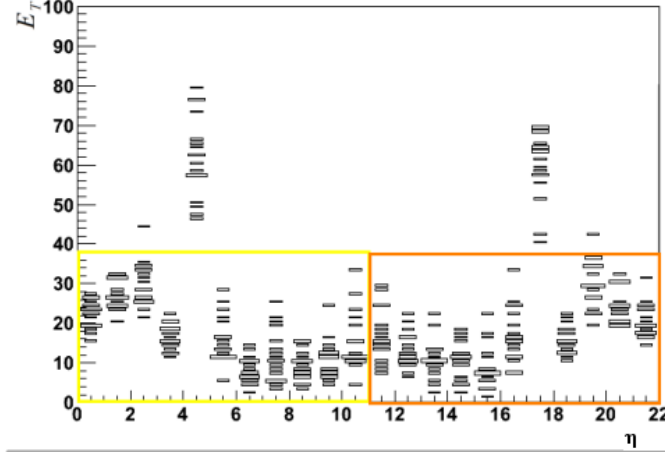


Figure 6: A representation of the failure mode of alternative algorithms using the current L1 hardware. Jets are found preferentially at $\eta=4$ and 17 in very central events (the eta value shifts with centrality) due to low p_T particles being swept into the endcaps. Background subtraction algorithms which operate within the RCT (either the yellow or the orange box) cannot reliably reduce the E_T at these η values. Lower p_T jets will still be present in the jet list, leaving the median or quartile values too low to reduce the impact of jets found at these η values. η -dependent background subtraction must be implemented which requires access to the full $\eta - \phi$ coverage of the calorimeter.

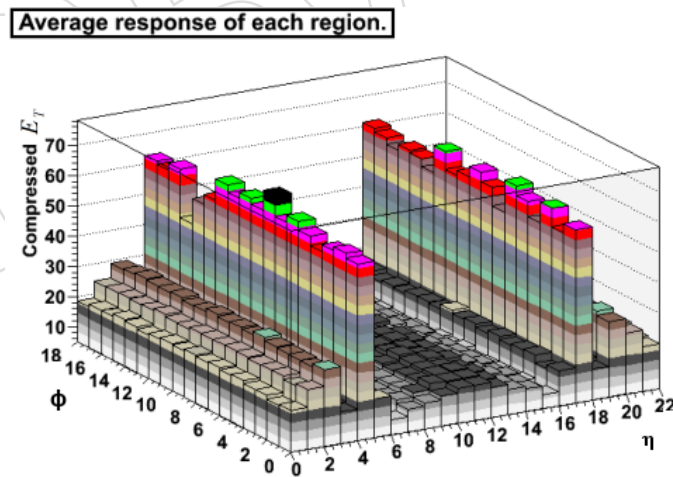


Figure 7: In support of Fig. 6, this is the average response of each region in a central sample. $\eta=4$ and 17 dominate the energy deposition in the calorimeter.

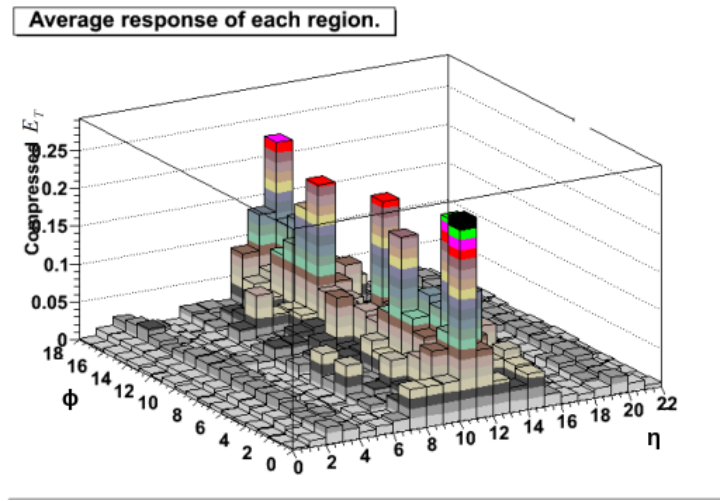


Figure 8: In support of Fig. 6, this is the average response of each region in a minimum bias sample. Most particles enter the calorimeter at mid-rapidity.

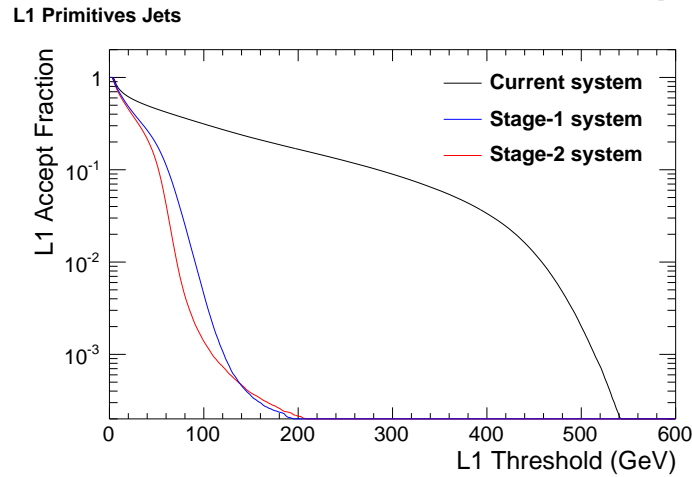


Figure 9: The jet finder is applied to minimum bias data from 2011 without event selection using the level-1 primitives present in the RAW data. The fraction of events which have a jet above a given E_t threshold is plotted as a function of that threshold. Note that the threshold is applied to the L1 jet energy and does not correspond to the HLT or offline jet energy scales.

3.3 Trigger Response (Jet Turn-On)

Another measure of the performance of the trigger is how efficient the trigger is at selecting jets above its threshold and rejecting those below the threshold; this is a jet turn-on curve. In a plot of accepted jets as a function of offline jet p_T (iterative cone calorimeter jets for this study), a performant trigger produces a sharp turn on from 0% accepted to 100% accepted. The offline jet p_T value at which the trigger is 100% efficient will not match the threshold value because of limitations in the jet definition at level-1; the figure of merit is the steepness of the curve.

In the case of heavy ion collisions, the difference in trigger performance as a function of centrality is important. A trigger may be performant at low centrality (low multiplicity) but inefficient at high centrality (high multiplicity).

All the following jet turn on curves are created using level-1 primitives and minimum bias data with event selection. Only events with $\geq 3\text{GeV}$ in each forward calorimeter are used. The sample is broken into two parts, one with centrality less than 30% and the other greater than 50%. For each event, the level-1 jet finder is run and the given threshold is applied. The fraction of events which pass the threshold as a function of the highest offline jet p_T (icPu5CaloJets) is plotted.

Current system.

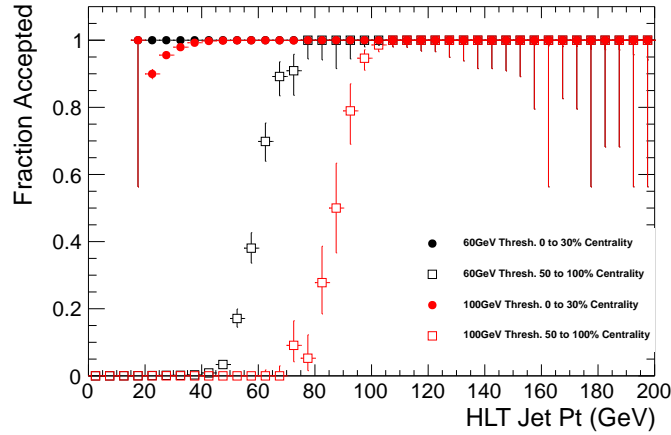


Figure 10: Jet turn on curves for the current system at an L1 threshold of 60 and 100GeV.

Stage-1 system.

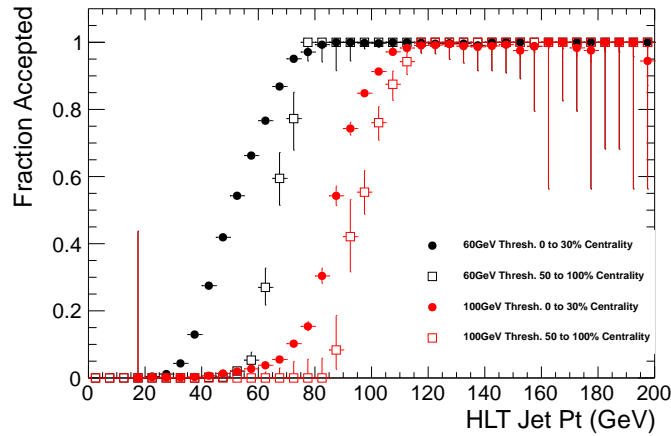


Figure 11: Jet turn on curves for the Stage-1 system at an L1 threshold of 60 and 100GeV.

3.4 Existing system

As can be seen from Figure 9, the existing trigger system requires a relatively high threshold value to reach the 5% accept rate required for the luminosity increase. At this threshold nearly all jets are rejected, severely limiting the physics capabilities of the detector.

Even at lower thresholds (with high dead-time in the high luminosity case), Figure 10 shows that the current system performs poorly for high centrality events.

Stage-2 system.

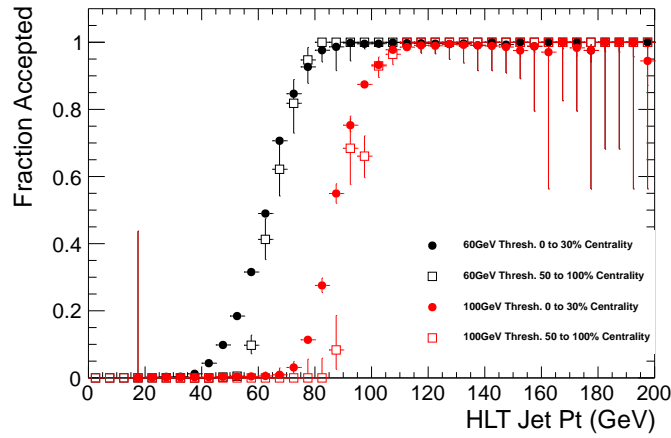


Figure 12: Jet turn on curves for the Stage-2 system at an L1 threshold of 60 and 100GeV.

3.5 Stage-1 system

Figure 9 shows that the required threshold for the Stage-1 system is relatively low, comparable to the full Stage-2 system. The jet turn-on curves, Figure 11, shows that the trigger is efficient and has closer performance between the high and low centrality samples, especially at the lower threshold. The Stage-1 system would adequately meet the requirements of the Heavy Ion program at the increased luminosity.

3.6 Stage-2 system

The most performant trigger, the full Stage-2 system is even more responsive to threshold changes than the 2015 system and shows nearly identical performance between the two centrality samples. The Stage-2 allows for more flexible level-1 trigger jet algorithms as well, including a single-tower trigger which could be used to look for high- p_T tracks to be used as seeds for other physics objects.

4 Track Trigger Performance

Figure 13 shows the performance of the track trigger in 2011 heavy-ion run. We were able to collect high p_T track sample with high efficiency. In this section, we investigated the possibility to use a L1 jet as a seed to reduce the L1 accept rate. The expected p_T reach of the tracks are also presented.

4.1 Projection to 2015 heavy-ion run

The expected p_T reach of charged particle spectra is also presented in Figure 14.

4.2 Performance with upgraded L1 system

With the upgraded L1 system and improved L1 jet trigger with underlying event subtraction, a much better correlation between the track p_T and L1 jet p_T can be achieved, as shown in Figure 15 (left) for 0–20% centrality and Figure 16 (left) for 60–100% centrality. Therefore, it is feasible to use high p_T L1 jet as a seed to the high p_T track high-level trigger. In this way, one can fully access the total delivered luminosity to significantly extend the track p_T reach in the high luminosity PbPb run (red markers in Figure 14), which is crucial for studying the

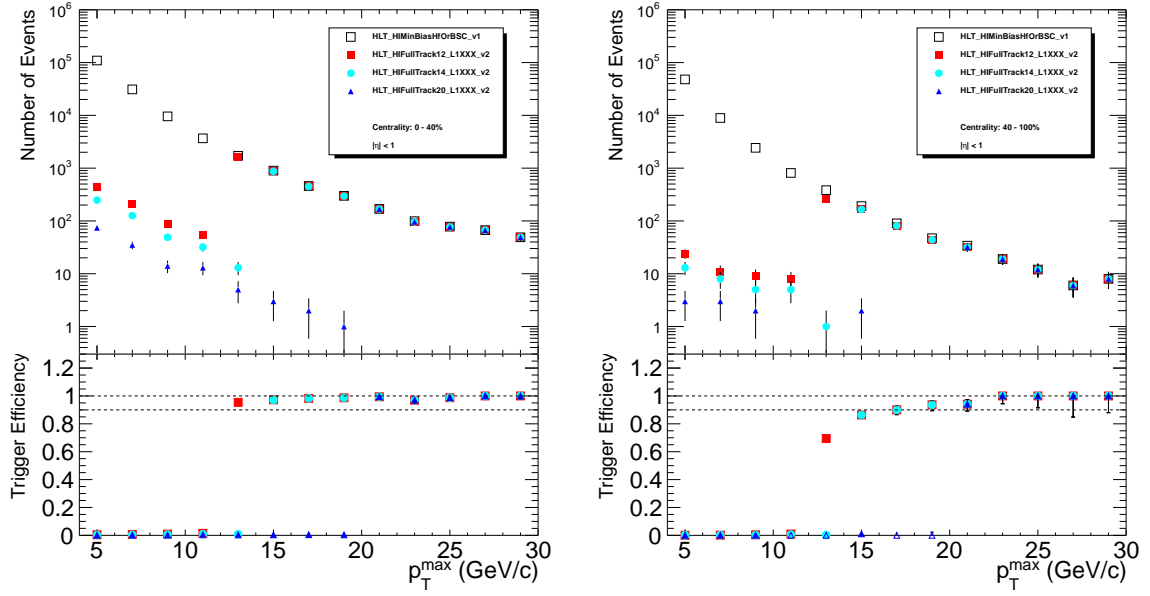


Figure 13: Track trigger performance in 2011 heavy-ion run. Leading track p_T distribution for track $|\eta| < 1$ in minimum-bias and triggered events for the 12, 14, and 20 GeV/c trigger threshold paths along with their efficiency (shown in the bottom) in 0-40% and 40-100% centralities.

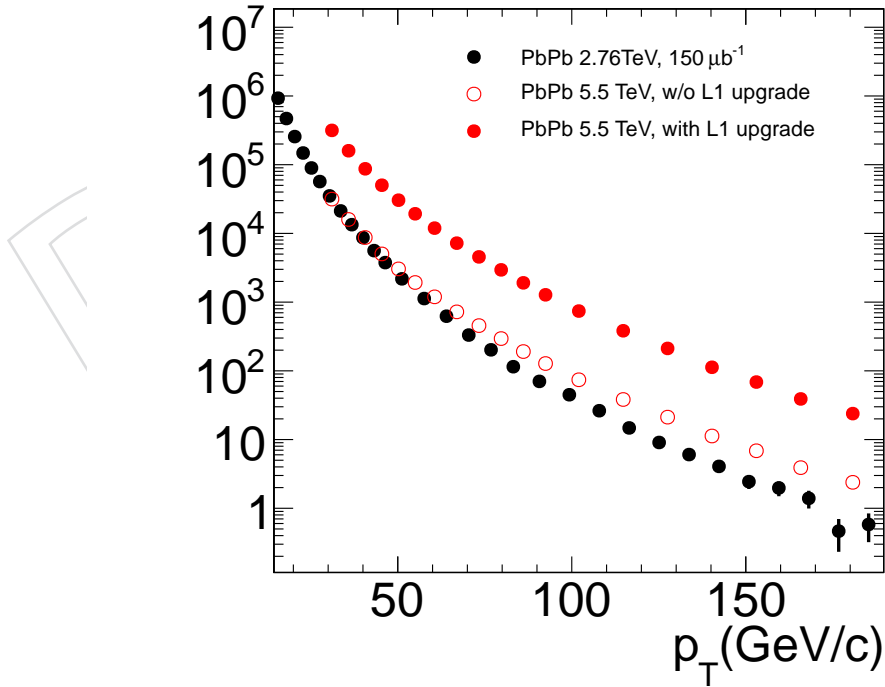


Figure 14: Track p_T distribution for 2.76 TeV PbPb in 2011 with a total integrated luminosity of $150\mu\text{b}^{-1}$ (solid black), projection to 5.5 TeV in 2015 based on x_T scaling without upgraded L1 trigger (open red), and with upgraded L1 trigger (solid red).

high p_T charged particle suppression and anisotropic azimuthal distribution. As shown on the right hand sides of Figure 15 and 16, by selecting L1 jet p_T of 40–50 GeV/c, one can maintain very high efficiency for the high p_T track trigger in both central ($>90\%$ for $p_T > 30$ GeV/c) and peripheral (100% for $p_T > 40$ GeV/c) heavy ion collisions, while the L1 jet rate can be controlled at a reasonable level.

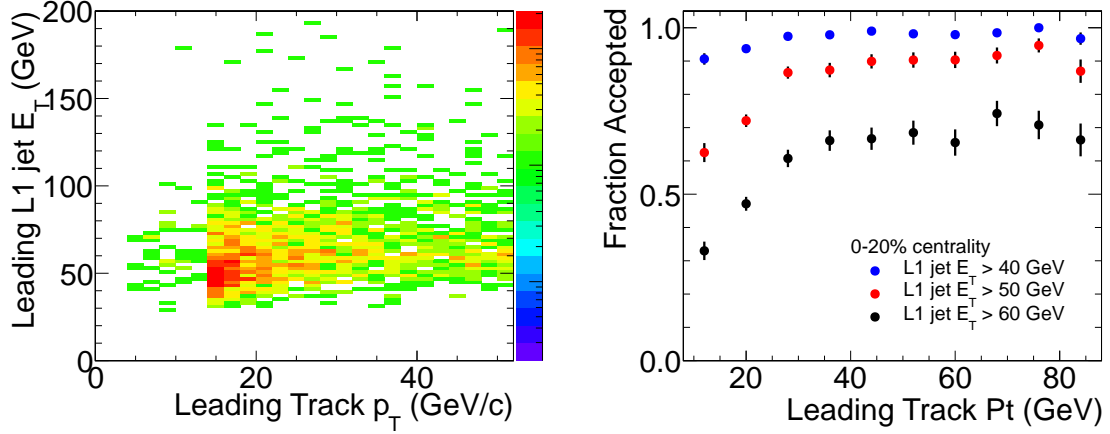


Figure 15: Leading L1 jet E_T , with upgraded L1 system, vs leading track p_T in 0-20% PbPb collisions at 2.76 TeV (left), and efficiency turn-on curve as a function of leading track p_T for L1 jet E_T thresholds of 20, 40 and 60 GeV (right).

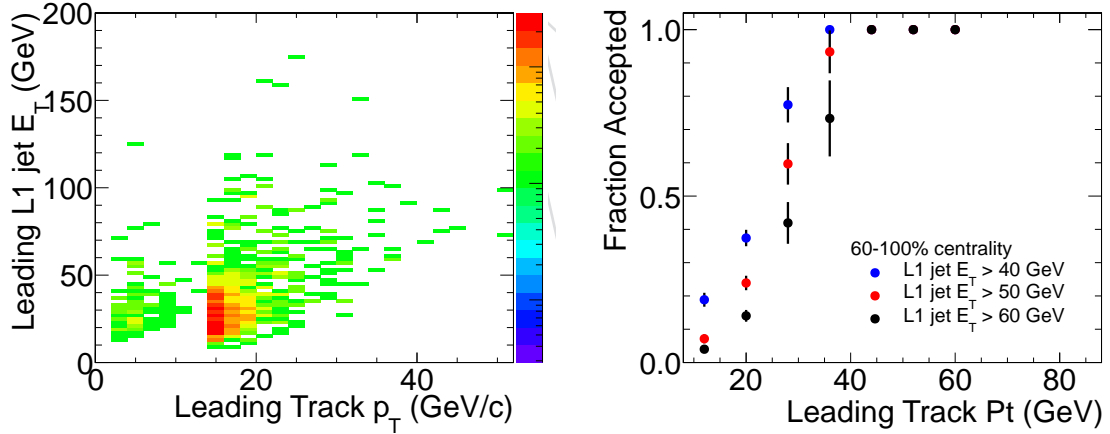


Figure 16: Leading L1 jet E_T , with upgraded L1 system, vs leading track p_T in 40-100% PbPb collisions at 2.76 TeV (left), and efficiency turn-on curve as a function of leading track p_T for L1 jet E_T thresholds of 20, 40 and 60 GeV (right).

5 Summary

The upgraded system will significantly improve the online jet trigger and it will be sufficient for data taking with heavy-ion collisions with increased luminosity and energy expected after the long shutdown LS1 and beyond. The intermediate (2015) system achieves similar performance for calo-jets as the SLHC system. With the upgraded system, studies of di-bjet asymmetry and 3-jet events are made possible and the p_T reach of the charged particle trigger is also extended from 100 GeV/ c to 160 GeV/ c .

DRAFT

References

- [1] CMS Collaboration Collaboration, “Observation and studies of jet quenching in PbPb collisions at nucleon-nucleon center-of-mass energy = 2.76 TeV”, *Phys.Rev.* **C84** (2011) 024906, doi:10.1103/PhysRevC.84.024906, arXiv:1102.1957.
- [2] CMS Collaboration Collaboration, “Jet momentum dependence of jet quenching in PbPb collisions at sqrt(sNN)=2.76 TeV”, *Phys.Lett.* **B712** (2012) 176–197, doi:10.1016/j.physletb.2012.04.058, arXiv:1202.5022.